Biophysical Chemistry 192 (2014) 1–9

Contents lists available at ScienceDirect

Biophysical Chemistry

journal homepage: http://www.elsevier.com/locate/biophyschem

Calculation of the volumetric characteristics of biomacromolecules in solution by the Voronoi–Delaunay technique

Vladimir P. Voloshin [a], Alexandra V. Kim [a], Nikolai N. Medvedev [a,b], Roland Winter [c], Alfons Geiger [c,*]

[a] Institute of Chemical Kinetics and Combustion, SB RAS, 630090 Novosibirsk, Russia
[b] Novosibirsk State University, 630090 Novosibirsk, Russia
[c] Fakultät für Chemie und Chemische Biologie, Technische Universität Dortmund, 44221 Dortmund, Germany

HIGHLIGHTS

- We retrieve the volumetric properties of a dissolved biomolecule by a Voronoi–Delaunay tessellation analysis of a molecular simulation run.
- The impact of the solute on the local density of the solvent is short ranged.
- The strong increase of the apparent volume with temperature is determined by the expansion of the extra void volume in the boundary region (the "thermal volume").

GRAPHICAL ABSTRACT

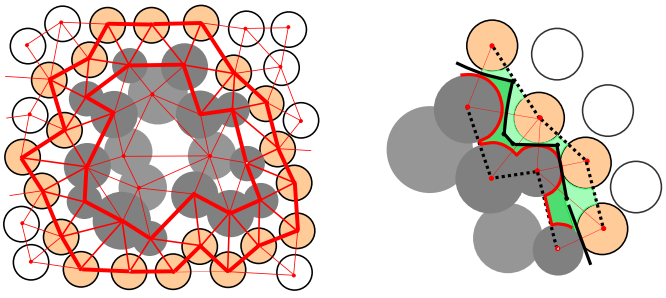

First Delaunay Shell Solute-Solvent Interface

ARTICLE INFO

Article history:
Received 11 April 2014
Received in revised form 15 May 2014
Accepted 15 May 2014
Available online 24 May 2014

Keywords:
Molecular dynamics simulation
Biomolecular solution
Voronoi–Delaunay tessellation
Boundary void
Apparent volume
Thermal volume

ABSTRACT

Recently a simple formalism was proposed for a quantitative analysis of interatomic voids inside a solute molecule and in the surrounding solvent. It is based on the Voronoi–Delaunay tessellation of structures, obtained in molecular simulations: successive Voronoi shells are constructed, starting from the interface between the solute molecule and the solvent, and continuing to the outside (into the solvent) as well as into the interior of the molecule. Similarly, successive Delaunay shells, consisting of Delaunay simplexes, can also be constructed. This technique can be applied to interpret volumetric data, obtained, for example, in studies of proteins in aqueous solution. In particular, it allows replacing qualitatively and descriptively introduced properties by strictly defined quantities, such as the *thermal* volume, by the boundary voids. The extension and the temperature behavior of the boundary region, its structure and composition are discussed in detail, using the example of a molecular dynamics model of an aqueous solution of the human amyloid polypeptide, hIAPP. We show that the impact of the solute on the local density of the solvent is short ranged, limited to the first Delaunay and the first Voronoi shell around the solute. The extra void volume, created in the boundary region between solute and solvent, determines the magnitude and the temperature dependence of the apparent volume of the solute molecule.

1. Introduction

The partial molar volume of a solute molecule, such as a protein in aqueous solution, is an important thermodynamic property, which contains interesting information about its structure and the interaction between solute and solvent. Moreover, according to Le Châtelier's

* Corresponding author. Tel.: +49 231 755 3937; fax: +49 231 755 3748.
E-mail addresses: voloshin@kinetics.nsc.ru (V.P. Voloshin), kim@kinetics.nsc.ru (A.V. Kim), nikmed@kinetics.nsc.ru (N.N. Medvedev), roland.winter@tu-dortmund.de (R. Winter), alfons.geiger@tu-dortmund.de (A. Geiger).

http://dx.doi.org/10.1016/j.bpc.2014.05.001
0301-4622/

principle, its changes upon reactions or conformational rearrangements determine the pressure dependence of the underlying chemical or structural equilibria. Changes in volume observed for conformational transitions in proteins are coupled to their other physico–chemical properties, such as expansibilities, compressibilities and volume fluctuations. Like them, the magnitudes of protein volume changes result from the specific amino acid sequence, and their characterization and understanding, likewise, yield important information about the physical basis for protein structure, stability and function. Specifically, the phenomenon of pressure-induced denaturation of proteins is accompanied by a decrease of its partial molar volume upon unfolding [1–5].

Generally, the void volume contributes significantly to the volumetric properties of proteins, and changes of temperature and pressure induce changes of the voids, both inside the solute molecule, at its boundary, and also in the surrounding water. However, using only experimental data, it is difficult to separate these contributions unambiguously. Computer simulations help to solve this problem. Models of the solutions are generated usually by molecular dynamics simulations (see for example Refs. [6,7]). The subsequent analysis of the models is aimed to detect and characterize interatomic voids and local densities.

There are very different approaches used for the analysis of voids in atomic and molecular systems. Some of them were developed for the investigation of the empty space between the atoms or particles in liquids and glasses [8–10], granular matters and colloids [11,12], polymers and membranes [13,14]. Others were designed to study cavities and pockets in large biological molecules [15–17]. Solvation shells [18,19] and the boundary region between proteins are also studied along these lines [20–22]. Consecutive shells, consisting of Voronoi cells, were used for the analysis of the density of hydration shells around polypeptides in Ref. [23].

In Ref. [22] we proposed an approach, where the voids both inside and in the surroundings of a solute molecule can be investigated by a single-stage method for all regions of the solution. It is based on the Voronoi–Delaunay method [24,25] which is a general mathematical tool for the detection and analysis of voids and the computation of local densities in any atomic and molecular system. In this work, we summarize shortly the main ideas of Refs. [22,23] to decompose the Voronoi–Delaunay tessellation of a solution into shells related to the solute. It allows characterizing voids (and thus the local density) both inside, at the solute–solvent boundary, and outside the solute molecule, and helps to analyze and discuss volumetric characteristics, in particular the *apparent* volume and its components.

The paper is organized as follows: In Sections 2–4 we shortly recapitulate the mathematical aspects of the method and introduce the shells, formed by Voronoi cells or Delaunay simplexes. In Sections 5 and 6 we apply this methodology to analyze the volumetric properties of a single polypeptide molecule in aqueous solution and to investigate its temperature-dependent behavior.

2. Voronoi–Delaunay tessellation of a solution

In molecular biology, Voronoi cells and Delaunay simplexes are known for a long time (see for example Refs. [26–32]). However, the tool becomes more powerful when we use a combination of both Voronoi cells and Delaunay simplexes in the so-called Voronoi–Delaunay tessellation [24,25].

Fig. 1 shows a two-dimensional illustration of a solution model and its Voronoi–Delaunay tessellation. It consists of a space-filling mosaic of Voronoi cells and the corresponding mosaic of Delaunay simplexes. Topologically, these mosaics are dual, and one of them can be produced from the other. Each Voronoi cell is assigned to a particular atom and represents the volume, which is closest to it. A Delaunay simplex represents the void space between mutually neighboring atoms.

Thus, in the following discussions of local densities and volumetric properties, one should keep in mind, that both tessellations are complementary, one is emphasizing the distribution of the occupied space, the other of the empty space.

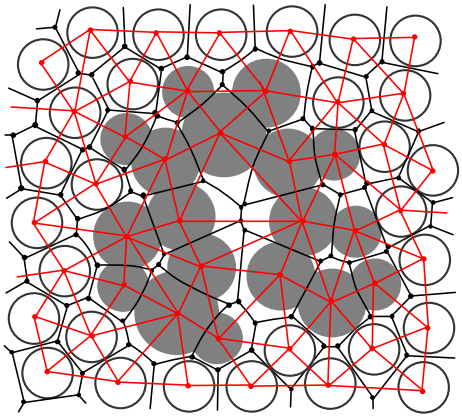

Fig. 1. 2D illustration of the Voronoi–Delaunay tessellation of a solution. Atoms of the solute molecule are shown by gray disks. Atoms of the solvent are light. Black lines show Voronoi cells, red lines show Delaunay simplexes.

Note, to study interatomic voids, the size of the atoms should be taken into account. As it is discussed in detail elsewhere [26–28,32], in this case the Voronoi cells should be constructed by referring to the surface of the atoms. Thus we should deal with the so-called *S-tessellation* [33,34] (or *additively weighted* Voronoi diagram) [24], instead of the ordinary Voronoi tessellation (which refers to the atomic centers [35,36]). S-tessellation gives a more physical assignment of the empty space to the atoms, as in this case a Voronoi cell comprises all points of space that are closer to the *surface* of a given atom than to the surfaces of all other atoms of the system. Voronoi S-cells have curved faces; this complicates the calculation of volumes. Other complexities of the S-tessellation (theoretically possible disconnectedness of the tessellation and overlapping of Delaunay simplexes in some cases) [25,37] are not important for our molecular systems, where the size difference of the atoms is rather small (usually the radii of the heavy or united atom spheres differ by not more than a factor of 2). Another variant, which considers the atomic surfaces, is the well-known *radical* (or *power*) tessellation [24,28,38]. In this case, the assignment of the empty space to individual atoms deviates slightly from the more physical S-tessellation, but it is much easier to implement.

We used both, the S- and the radical tessellation, and found that the obtained volumes do not differ very much, yielding the same physical results [23]. In this paper we use the radical tessellation, because an efficient method for the calculation of the empty volume of the intersection of Voronoi and Delaunay shells (see below) was implemented only for this tessellation [39].

In our geometrical analysis, the molecules of the solvent (the water molecules) are considered as uniform spheres, which are centered on the oxygen atom, as it is usually done in structural analyses of computer models of water and aqueous solutions. The atoms of the solute molecule are considered as spheres with diameters equal to the values of their Lennard-Jones parameters σ, used in the molecular dynamics simulations.

The calculation of the Voronoi–Delaunay tessellation is straightforward now. Here we used our own algorithms, but programs for the calculation of power tessellations are available also in standard geometrical libraries [40].

In a first stage, no distinction between solute and solvent atoms is made: the system of all atoms is considered as a whole. The tessellation is calculated for a large number of instantaneous configurations ("snapshots") of the simulation run, to yield the mean values of the studied characteristics.

3. Voronoi shells

Knowing the adjacency of the atoms from the Voronoi–Delaunay tessellation, one can begin to allocate Voronoi shells around the solute molecule. At first, the boundary Voronoi shell of the solute molecule is constructed by use of the following simple rule: *go over all atoms of the solute molecule and mark those, which are adjacent to at least one atom of the solvent (adjacency is defined by the sharing of a common Voronoi face)*. Thus we establish the set of atoms of the solute molecule, which are in direct contact with the solvent, and simultaneously, the set of atoms of the solvent which are in contact with the solute. The former represent the boundary atoms of the solute, and the latter define the nearest solvation shell.

Let us assign indexes 0 and 1 to these atoms, and call these groups of atoms (and their Voronoi cells) as *0th* and *1st Voronoi shell* (see Fig. 2). Let us denote the number of atoms in the shells as N_0 and N_1. The volume of the shells (V_0 and V_1) can be calculated as the sum of the volumes of the Voronoi cells in a given shell.

Knowing the 1st Voronoi shell, one can calculate all outer shells. The 2nd Voronoi shell is defined by the solvent atoms which are neighbors of the 1st shell (adjacent to atoms with index 1). Let us assign index 2 to these atoms. Similarly, we can select outer neighbors of the 2nd shell. They define the 3rd Voronoi shell and get index 3. By continuing further, all subsequent Voronoi shells can be selected, and called the 4th, 5th, …, *k*th … and so on, up to the maximum that is permitted by the size of the model system [22,23]. From a mathematical point of view, the Voronoi shells correspond to the consecutive topological neighbors on the Delaunay network (Fig. 1, see for example Ref. [41] and references given there). However, in those papers the selection of the neighbors begins from a single (central) site (Voronoi cell). In our case, we start from the boundary atoms of the solute molecule. The shapes of the Voronoi shells can be very different and are determined by the structure and conformation of the solute molecule.

In Ref. [22] it was proposed to continue the construction of Voronoi shells into the interior of the molecule. All internal neighbors of the 0th shell represent the −1st *(minus first)* Voronoi shell. The atoms of this shell have index −1. Similarly, one can select inner neighbors of the −1st shell. They represent the −2nd (*minus second*) Voronoi shell, and its atoms get the index −2. By continuing this, one can determine all subsequent "negative" shells, until all atoms of the molecule are covered.

Thus, we decomposed the solution into shells in relation to the surface of the solute molecule. This decomposition is unambiguous: no atom (Voronoi cell) is unconsidered, and none is taken into account twice. For each Voronoi shell different characteristics can be calculated, e.g.: the number of atoms N_k (the number of Voronoi cells); the volume V_k, defined as the sum of the volumes of all Voronoi cells of the shell; the mean volume of the Voronoi cell $v_k = V_k/N_k$; the inner and outer surface areas S_{k-1} and S_k, which are calculated as the sum of the areas of the Voronoi faces that are shared by the atoms of adjacent shells, and so on.

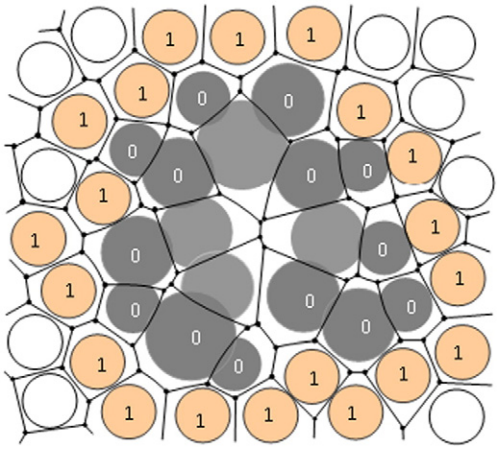

Fig. 2. Illustration of the 1st and the 0th Voronoi shell. All solvent atoms with index 1 (pink circles) have at least one atom of the solute as a neighbor. All solute atoms with index 0 (dark-gray circles) have at least one atom of the solvent as a neighbor.

4. Delaunay shells

We can classify the Delaunay simplexes of the solution by using the indexes of the Voronoi shells. Let us define thus the *index I of a given Delaunay simplex* as the sum of the Voronoi shell indexes i_k of the atoms at its vertices [22] (recall: a Delaunay simplex has four vertices in 3D): $I = i_1 + i_2 + i_3 + i_4$.

Atoms of the 0th ($i_k = 0$) and the 1st ($i_k = 1$) Voronoi shell can form the following simplex indexes:

$I = 0$ (all simplex vertices are located on atoms of the solute molecule: all $i_k = 0$);

$I = 1$ (three vertices on the solute and one on solvent: one $i_k = 1$);
$I = 2$ (correspondingly: two $i_k = 1$);
$I = 3$ (correspondingly: three $i_k = 1$);
$I = 4$ (all vertices are on solvent molecules: all four $i_k = 1$).

We call the union of Delaunay simplexes with the same index I as *Delaunay subshell I*. The subshells 0 and 4 are produced by atoms that belong to the same Voronoi shell (the 0th, and the 1st one). They are the result of "folds" ("wrinkles") of the Voronoi shells, and typically they contain less simplexes and their volume is smaller than that of neighboring subshells. For our current task more important are the subshells, which are formed by Delaunay simplexes with vertices both from the 0th and 1st Voronoi shells ($I = 1, 2, 3$). The union of these simplexes represents a solid shell between the solute and the solvent. We call this shell the *first Delaunay shell.* (To emphasize a distinction between shells of Delaunay simplexes and shells of Voronoi cells, we used in Refs. [22,23] the word "layer" in case of Delaunay simplexes. Here and afterwards we use the word "shell" in the both cases.)

For illustration, Fig. 3 shows the first Delaunay shell in two dimensions. In the plane, the Delaunay simplex has three vertices, thus $I = i_1 + i_2 + i_3$ with $i_k = 0$ or 1. Then there are only four different Delaunay simplex indexes: $I = 0$–3, and the first Delaunay shell is composed of two Delaunay subshells ($I = 1$ and 2).

As it was discussed in Ref. [22], one can also define subsequent Delaunay shells, between consecutive Voronoi shells. The simplexes, whose vertices are positioned on atoms of the first and the second Voronoi shells, represent a solid shell between the atoms of these Voronoi shells, and define the *second* Delaunay shell, and so on. We can also select Delaunay simplexes inside the solute molecule. They

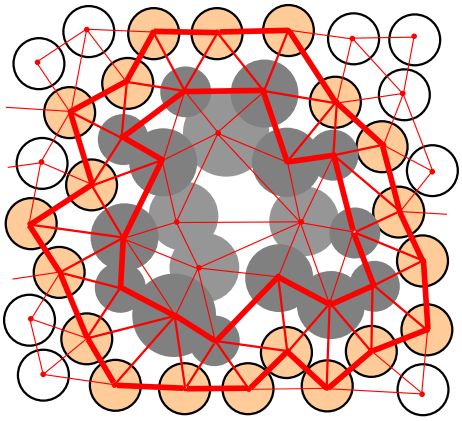

Fig. 3. 2D illustration of the first Delaunay shell for the model shown in Fig. 2 (between thick red lines).

form the inner Delaunay shells with numbers 0 (zero), −1 (minus one), −2 (minus two) and so on. Every K-th Delaunay shell can be characterized by its total volume D_K or by its empty volume E_K (without the volume occupied by the spheres, which represent the atoms). Below we will deal mainly with the first Delaunay shell, which represents the boundary area between the solute molecule and the solvent.

5. Voronoi and Delaunay shells in an aqueous solution of the hIAPP molecule

In this paper we analyze molecular dynamics simulations of an aqueous solution of a polypeptide molecule, which is essentially unfolded in its native state, the human islet amyloid polypeptide (hIAPP). The simulation runs had been produced by Andrews and Winter [42]. The system consists of a single solute hIAPP molecule, containing 462 heavy atoms, which is surrounded by 10843 SPC/E water model molecules (for more simulation details, see Ref. [42]). Production runs of up to 500 ns each had been performed for 11 different temperatures from 250 to 450 K. For the analysis of the individual simulation runs, 1000 independent snapshots, equally spaced over the last 200 ns (every 200 ps) were used for averaging the volumetric properties.

These models had been used also in our previous paper, Ref. [23], where we discussed methods for the selection of hydration shells and investigated different approaches for the calculation of the apparent volume of a solute macromolecule. Here we extend the volumetric analysis to a more detailed level: we analyze voids both in the surrounding water and in the interior of the biopolymer, calculate separate contributions to the apparent volume and relate them with distinct components of the empty boundary volume.

We decompose the configurations of the molecular dynamics runs into Voronoi and Delaunay shells, as described above. The size of our system allows the use of seven consecutive Voronoi shells: $k = -1, 0, 1, 2, 3, 4, 5$. The shell −2 appears not in every configuration, therefore we do not analyze it specially.

Fig. 4 (left) shows the temperature dependence of the volumes of the Voronoi shells number $k = -1, 0, 1$ and 2. With the exception of shell $k = -1$, the shells demonstrate a pronounced increase of the volume with temperature. It reflects obviously the decrease of the bulk water density with temperature (see Fig. 5). The kinks in the curves of the shell volume V_k in Fig. 4 is due to an insufficient sampling. There are similar kinks in the curves for the number of cells in the shells N_k (see Fig. 10 in Ref. [22]). However, the curves becomes more smoothed, when we go from the volume of the shells to the density N_k/V_k (see Fig. 6).

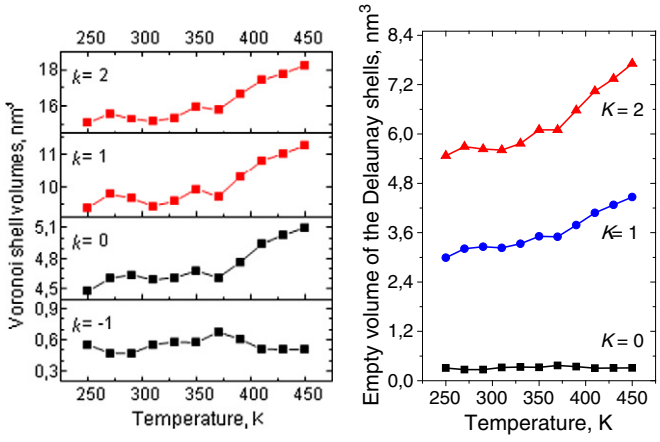

Fig. 4. (Left) Voronoi shell volumes of the hIAPP molecule in aqueous solution as a function of temperature. From bottom to top: shells numbers −1 to 2. (Right) Empty volume of the Delaunay shells for the same molecule.

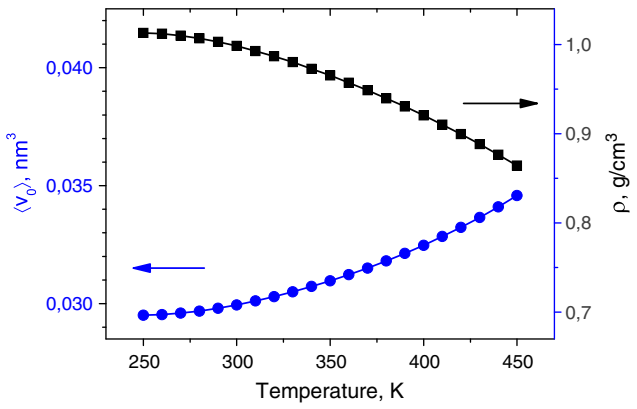

Fig. 5. Temperature behavior of the density of bulk SPC/E water, used in the simulation (squares, right axis), and the mean volume of the Voronoi cells of the bulk water molecules, $\langle V_0 \rangle = 1/\rho$ (circles, left axis). Note that the density maximum of the SPC/E water model is close to 240 K [43].

For the inner Voronoi shell ($k = -1$), there is no noticeable change with temperature. This means that the dissolved molecule itself does not change its volume systematically. The same is shown for the Delaunay shells: the empty volume E_K of the inner Delaunay shell ($K = 0$) does not change with temperature, whereas the empty volume of the boundary ($K = 1$) and the outer one ($K = 2$) increase (see Fig. 4, right).

Fig. 6 shows the relative density $\rho_k/\rho_{\text{bulk}}$ of water in different Voronoi shells (from 1st to 4th) as function of temperature. The density ρ_k of the kth shell is defined in this case as the ratio N_k/V_k, where N_k is the mean number of water molecules, and V_k is the mean volume of the kth shell. A significant difference to bulk water is observed only for the first Voronoi shell ($k = 1$): between 4% and 1% in our temperature interval. This increased local density is in accord with the generally observed existence of a pronounced peak in the water density distribution around a solute molecule [23]. In the next shells, the water density is very close to the bulk value for all temperatures. In this case the deviation of the ratio from 1 is at the limits of our computational uncertainty. However, the density in the second shell appears to be slightly higher than in the third and fourth shells. Thus one can say that the solute molecule slightly influences also the second shell of the hydration water.

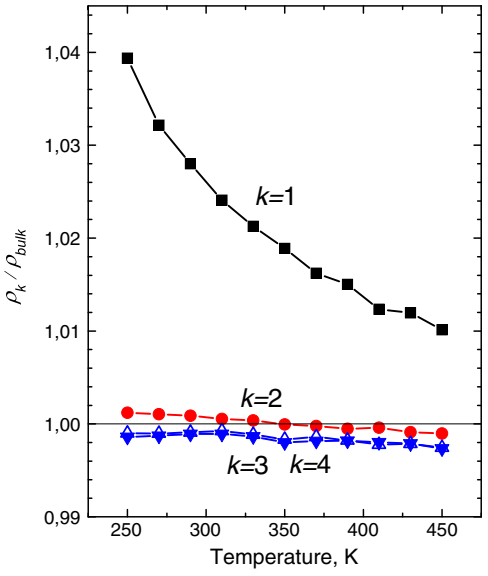

Fig. 6. Relative density of water in different Voronoi shells with respect to bulk water at the same temperature, $\rho_k/\rho_{\text{bulk}}$. The shells vary from 1st to 4th.

We remind here the following technical detail: when calculating the mean volume of Voronoi shell V_k, the so-called mosaic effect (due to the existence of a correlation between the volume of a Voronoi cell and the number of its neighbors) should be taken into account [23,44]. This correlation leads to a small artificial overestimation (in the range of one percent) of the mean volume of the Voronoi shells. The necessary corrections were done by using the formulas suggested in Ref. [44]. The small shifts of the relative densities of the third and fourth shells to values below 1.0 in Fig. 6 presumably results from the approximate nature of these corrections.

6. Apparent volume and its components

The partial molar volume of a solute molecule *j* in aqueous solution is defined as the volume change of the solution, when the solute is added: $V_j = (\partial V/\partial N_j)_{T,p,Nw}$, where N_j and N_w are the number of solute and solvent molecules, respectively. At infinite dilution, i.e. without contribution of solute–solute interactions, the volume change on adding a single solute molecule to the solvent is called the *apparent* volume V_{app} of the solute molecule in the solvent.

Generally, it is assumed that V_{app} is given by the sum of two contributions, the *intrinsic* volume V_{int}, which reflects the "size" of the solute molecule in solution, and a volume change ΔV in the surrounding solvent [1,45–47].

$$V_{app} = V_{int} + \Delta V \tag{1}$$

Eq. (1) should also contain an ideal gas term, but this can be neglected due to the low compressibility of water [1,47–49].

Unfortunately there is no experimental method, which allows a separation of the two component volumes V_{int} and ΔV and theoretical approaches slightly vary in different papers.

6.1. Intrinsic, molecular, and thermal volume

In the framework of a Voronoi–Delaunay analysis it is natural to equate the intrinsic volume V_{int} of a molecule with its *Voronoi volume* (V_{Vor}). The Voronoi volume is the volume "assigned" to the solute molecule in solution, and can be calculated as the sum of the Voronoi volumes of all atoms of the molecule. It includes the van der Waals volume (the sum of all fused spheres, representing the atoms of the solute molecule), the empty space inside, and a part of the surrounding empty space (see Figs. 2 and 7). This was discussed in biological physics many times [23,27,29,30]. The calculation of the Voronoi volume of a molecule can be performed from molecular dynamics models without problems. Thus we suggested in Ref. [23] that

$$V_{int} = V_{Vor}. \tag{2}$$

In Refs. [50–52] the *cavity volume* V_{cav} is introduced, which is the volume accommodating the solute molecule and is assumed to consist of two parts:

$$V_{cav} = V_M + V_T. \tag{3}$$

V_M is the *molecular volume* and is assumed to be the van der Waals volume of the solute molecule, together with the volume of inner voids, both impenetrable to the surrounding water. To calculate V_M, we should first define a complete boundary around the molecule. Usually, the well-known Connolly surface [53] is used for this purpose. However this needs the introduction of an extra parameter *R*, the radius of a probe sphere rolling over the molecule. Within the Voronoi–Delaunay technique, a similar surface can be provided without any additional parameter. This *molecular surface* consists of segments of atomic surfaces (parts of spheres) and sections of the Delaunay simplex faces (parts of planes), covering the gaps between boundary atoms (see bold red line in Fig. 7 as two-dimensional illustration). The volume inside this surface can be calculated as the volume of the union of all atoms of the molecule, plus the empty volume of all Delaunay simplexes, which are formed by the atoms of the solute molecule [39].

V_T is the so-called *thermal volume*, which represents an extra void volume around the solute molecule. As written in Refs. [1,47], it is the "void volume created around a solute molecule due to the mutual vibrations of solute and solvent molecules as well as to structural, packing, and steric effects." This interpretation does not really give a recipe to trace out this volume. In Refs. [50–52] it is considered as an empty shell around a solute molecule with thickness δ. This is a formal description of the voids appearing around the solute molecule, and the value of δ is a measure for the thermal volume in the frame of this theoretical approach.

6.2. Empty boundary volume V_B

The Voronoi–Delaunay method, equipped with mathematically strict definitions, helps to investigate the surrounding voids in detail. Firstly, we calculate the *empty boundary volume* V_B as the sum of the empty volumes of the Delaunay simplexes, which form the first Delaunay shell (dark and light green areas in Fig. 7).

The calculation of the empty volume of the Delaunay simplexes for overlapping atoms can be done both by numerical and analytical methods (see for example Refs. [14,39]). Obviously, we cannot equate V_B strictly with the thermal volume V_T, because the latter one is not defined geometrically. Nonetheless, the temperature behavior of V_B and V_T should be closely related. Thus we can examine V_B to investigate the role of the solute–solvent boundary in the temperature dependence of the apparent volume.

The empty boundary volume V_B is divided into two parts by the Voronoi surface of the molecule (Fig. 7):

$$V_B = V_B^M + V_B^S. \tag{4}$$

The first part (V_B^M) is assigned to the solute molecule and the second one (V_B^S) belongs to the solvent. The volume calculation of these individual components is more complex (they are intersections of the Delaunay and Voronoi shells), however, it can be also performed by our method [39].

Fig. 8 demonstrates the temperature behavior of the boundary empty volume V_B and its components for the hIAPP molecule. We see a strong (around 50%) temperature change in the considered

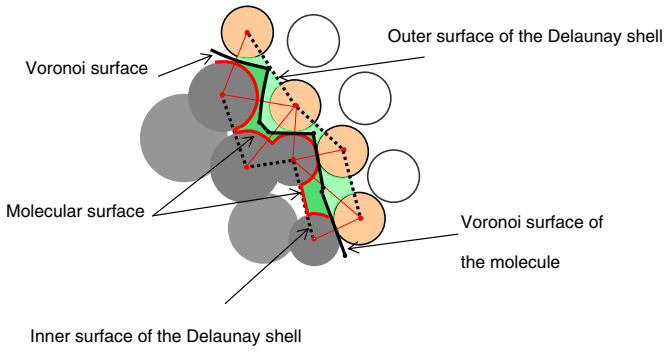

Fig. 7. A section of the model shown in Fig. 2. Dotted lines show the inner and outer surfaces of the first Delaunay shell. The black thick line shows the *Voronoi surface* of the solute molecule. It confines the *intrinsic volume* of the solute molecule. The empty volume of the Delaunay shell (V_B) is green. The dark-green part is assigned to the solute molecule (V_B^M). The light-green area belongs to the solvent (V_B^S). The thick red line around the atoms of the molecule represents the Voronoi–Delaunay *molecular surface*, which confines the *molecular volume* V_M of the solute molecule.

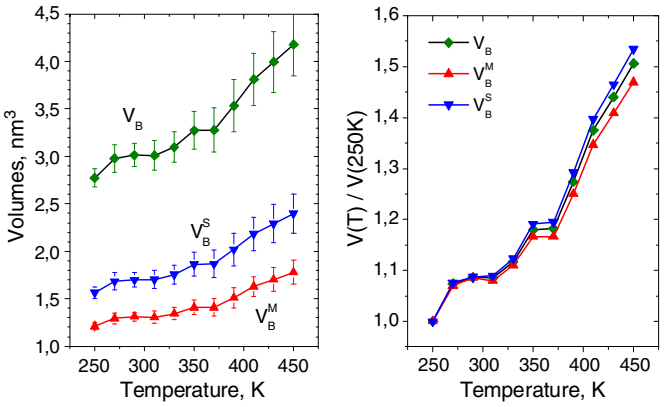

Fig. 8. Left: Empty volume of the boundary region between the hIAPP polypeptide and the solvent (V_B, diamonds). V_B^M (triangles): the part of V_B, which is assigned to the solute molecule; V_B^S (inverted triangles): the part of V_B, which is assigned to the solvent. Right: the same data, but normalized by the corresponding values at 250 K.

temperature range. Note, the normalized change of these volumes is identical (see Fig. 8, right). This means that the division of V_B into V_B^M and V_B^S is rather mathematical than physical. Both components are equivalent parts of the boundary empty volume.

It is most interesting that the magnitude of the thermal expansion of V_B, (about 50%) is much larger than that of the pure model water, which is less than 20% in the same temperature interval (see Fig. 5). Thus the density in the boundary region decreases with temperature much stronger than in bulk water. This is an indication that the boundary region dominates the temperature dependence of the apparent volume in Fig. 9.

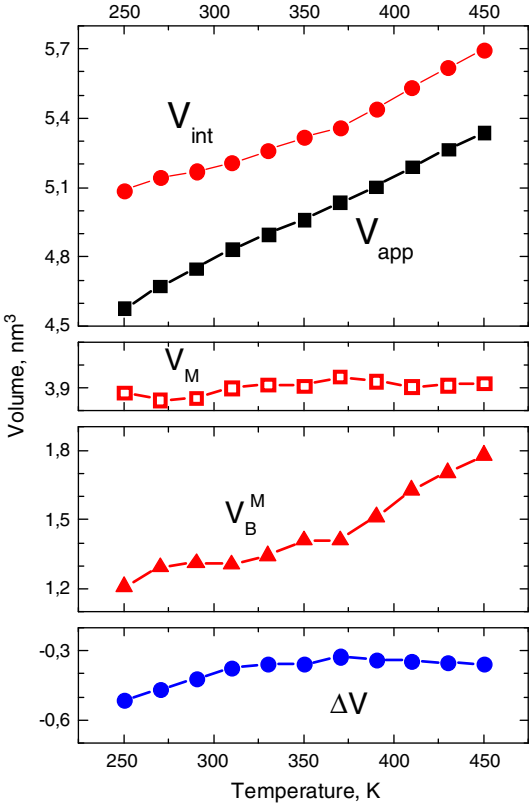

Fig. 9. Apparent volume V_{app} of the polypeptide hIAPP in water and its components as function of temperature. $V_{int} = V_M + V_B^M$: intrinsic volume calculated as Voronoi volume of the molecule; V_M: molecular volume, V_B^M: boundary empty volume assigned to the solute molecule. ΔV: contribution of the solvent calculated as ($V_{app} - V_{int}$).

6.3. Decomposition of the apparent volume

The apparent volume V_{app} of the hIAPP molecule had been calculated previously [23]. Remember, V_{app} is the difference between the volume of the solution and the volume of the same amount of pure solvent. In the simplest case, it can be calculated as the difference between the volume of a model box with the solute molecule in water, and the volume of the model box, containing the same amount of pure water at the same pressure and temperature. Different approaches to determine V_{app} are discussed in Refs. [23,46,48,49,54].

On the other hand, using Eqs. (1) and (2) and the relation

$$V_{Vor} = V_M + V_B^M \tag{5}$$

which is obvious from Fig. 7, we can present the apparent volume as:

$$V_{app} = V_M + V_B^M + \Delta V. \tag{6}$$

Fig. 9 assembles the temperature behavior of the apparent volume and its components, calculated for the hIAPP molecule. The values of V_{app} and $V_{int} = V_{Vor}$ were calculated earlier in Ref. [23]. Now we demonstrate also the temperature dependence of V_M and V_B^M.

We see, V_M does not change with temperature, whereas V_B^M and ΔV increase markedly. (The latter quantity was determined according to Eq. (1) as difference between the calculated values V_{app} and $V_{int} = V_{Vor}$). Thus, here the temperature behavior of the apparent volume is caused by V_B^M and ΔV, but not by V_M.

Note that ΔV is negative. This is because in the partitioning of V_{app} according to Eq. (6) ΔV mainly reflects the increased density of the first Voronoi shell around the hIAPP molecule (see Fig. 6). With increasing temperature the density of the first Voronoi shell decreases. However, it remains larger than in the bulk up to the highest temperatures considered here.

6.4. Estimation of ΔV

From the definition of the apparent volume, the contribution of the solvent ΔV can be written as [23,46,54]:

$$\Delta V = V^{hyd} - V^{bulk}, \tag{7}$$

where V^{hyd} is the volume of the "hydration water" (all the water that is influenced by the solute molecule) and V^{bulk} is the volume of the same amount of bulk water. As the "van der Waals volume" of the individual water molecules is fixed, ΔV is fully determined by the change of the void volume. Thus ΔV is given by the difference between the void volume in the hydration water (V_{void}^{hyd}) and the void volume in the same amount of bulk water (V_{void}^{bulk}). As V_{int} in Eq. (1) is bounded in our approach (Eq. (2)) by the Voronoi surface (Fig. 7), the hydration volume V^{hyd} extends to the Voronoi surface of the solute molecule. Thus, the voids in the hydration water can be written as the sum of the part V_B^S of the empty boundary volume V_B that is outside the Voronoi volume (see Fig. 7 and Eq. (4)), plus the volume of the voids in the hydration water beyond V_B ("the rest"):

$$V_{void}^{hyd} = V_B^S + V_{void}^{rest,hyd}. \tag{8}$$

Formally, a similar expression can be written for the voids in bulk water:

$$V_{void}^{bulk} = V_B^{S,bulk} + V_{void}^{rest,bulk}. \tag{9}$$

Here, $V_B^{S,bulk}$ is the void volume of a water layer in bulk water, which is comparable to the volume V_B^S.

After subtraction we get

$$\Delta V = V_{void}^{hyd} - V_{void}^{bulk} = \left(V_B^{S} - V_B^{S,bulk}\right) + \left(V_{void}^{rest,hyd} - V_{void}^{rest,bulk}\right).$$

As the density beyond the first Voronoi shell of our solute molecule is practically identical to that of bulk water (Fig. 6), we may assume that

$$V_{void}^{rest,hyd} - V_{void}^{rest,bulk} \approx 0, \quad (10)$$

and therefore

$$\Delta V \approx V_B^{S} - V_B^{S,bulk}. \quad (11)$$

From our calculations we know ΔV and V_B^S (Figs. 8 and 9), so we can estimate from Eq. (11) the value of $V_B^{S,bulk}$. Fig. 10 demonstrates the temperature behavior of the components of Eq. (11). The fact, that the empty boundary volume V_B^S is smaller than the void volume $V_B^{S,bulk}$ of a comparable amount of bulk water (in accord with the higher density of the first Voronoi shell), leads to the negative value of ΔV.

$V_B^{S,bulk}$ can be estimated as a part of the void space of n_1 water molecules in bulk water, where n_1 is the number of water molecules in the first Voronoi shell of our solute molecule. It can be written as

$$V_B^{S,bulk} = f \cdot v_0^{empty} \cdot n_1, \quad (12)$$

where the factor f should be about 0.5. Indeed, the product $v_0^{empty} \cdot n_1$ estimates the mean empty volume of the first Voronoi shell, and the volume $V_B^{S,bulk}$ corresponds to the inner half of this shell: the light green area in Fig. 7, bounded by the outer surface of the first Delaunay shell (dotted) and the Voronoi surface (black thick line). The mean empty volume per molecule in bulk water v_0^{empty} and the mean number of water molecules in the Voronoi shell depend on temperature and can easily be calculated in our approach (see Ref. [22] and Fig. 5). We found that the factor f does not depend on temperature and is equal to 0.452 ± 0.004. The crosses in Fig. 10 show the validity of Eq. (12). (This coincidence confirms the correctness of our reasoning to use the formal decomposition of V_{void}^{bulk} in Eq. (9) and of the estimate Eq. (10)).

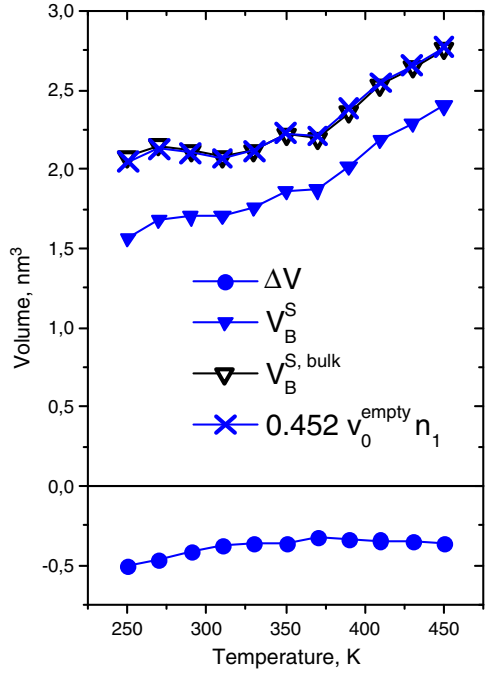

Fig. 10. Temperature behavior of the components of Eq. (11): ΔV (circles), V_B^S (triangles), $V_B^{S,bulk}$ (empty triangles). Crosses show values $0.452 \cdot v_0^{empty} \cdot n_1$, see text.

6.5. Alternative decomposition of V_{app} : V_B as the "themal volume"

In spite of the fact that the volume V_B is not an explicit component of the apparent volume in Eq. (6), this quantity is most suitable to represent the thermal volume as introduced in Refs. [1,47], where it was defined as the void between solute and solvent molecules. To explicitly connect it with the apparent volume, we write, by using Eqs. (11) and (6):

$$V_{app} = V_M + V_B - V_B^{S,bulk}. \quad (13)$$

This partitioning of V_{app} points out, that the extra volume contribution beyond the impenetrable molecular volume V_M is constituted by the void volume V_B between the molecule and the solvent, corrected by the void volume $V_B^{S,bulk}$, which had already been present in the bulk water, as discussed above.

Fig. 11 demonstrates the temperature behavior of the components of Eq. (13) for the hIAPP molecule. We can say, that the increase of V_{app} with temperature is caused solely by the expansion of the extra void volume $V_B - V_B^{S,bulk}$, induced by the solute molecule in its close vicinity.

The fact, that the apparent volume V_{app} of the hIAPP molecule increases, means that the empty volume in the boundary region expands with temperature faster than in the bulk. This property is quite general. In fact, experimental investigations of water in porous materials as well as simulations of water in cylindrical and slit model pores with structure-less hydrophilic and hydrophobic walls have shown, that the thermal expansion coefficient of hydration water at ambient temperatures is larger than that of bulk water [55]. This has been assigned to the reduced number of water neighbors at the interface.

Finally it should be noted, that the depleted region, which envelopes the solute molecule, is very thin, it does not extend beyond the first Delaunay shell. This is in accord with the small values, given in the literature for the "empty shell" thickness [50–52].

7. Conclusions

In this paper we use the decomposition of the molecular dynamics models of a biomolecular solution into Voronoi and Delaunay shells,

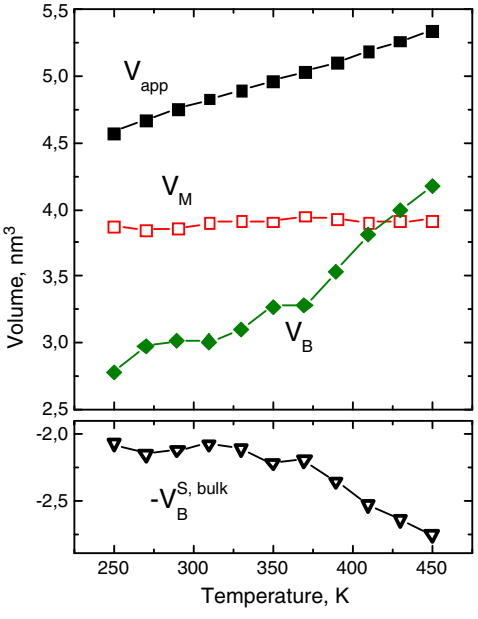

Fig. 11. Apparent volume V_{app} of the polypeptide hIAPP in water and its components as function of temperature. V_M: molecular volume, V_B: total boundary empty volume between the solute molecule and solvent, $V_B^{S,bulk}$: contribution from bulk water, see text.

as discussed in Ref. [22], to study the temperature behavior of the apparent volume of a natively unfolded polypeptide (hIAPP) in aqueous solution. In the first stage, the Voronoi–Delaunay tessellation is calculated for the total ensemble of atoms of the solution. After that, consecutive Voronoi and Delaunay shells are defined, starting from the border between molecule and solvent. We use this approach to make a quantitative calculation of the molecular volume of the solute (V_M – volume of the union of atoms of the molecule together with the inner voids) and the empty volume at the boundary region between solute and solvent (V_B – empty volume of the boundary Delaunay shell). Additionally, we separate this empty volume into two parts, which are assigned to the solute (V_B^M) and the solvent (V_B^S), respectively. The impact of the solute on the local density of the solvent is very short ranged, limited to the first Delaunay and the first Voronoi shell around the solute. A depletion zone, represented by the inner part V_B^M of the first Delaunay shell is followed by a zone of increased density, represented by the first Voronoi shell.

We show that the strong increase of the apparent volume of hIAPP with temperature is mainly due to the expansion of the surrounding boundary layer (V_B), but not to the modification of the solute molecule itself. The molecular volume V_M does not change perceivably with temperature. Additionally, it was found that the contribution of the solvent beyond the boundary layer to the temperature dependence of the apparent volume of hIAPP is negligible.

It is safe to say that the characteristics and the temperature dependence of the apparent volume of hIAPP is largely controlled by the "thermal volume," a term often discussed in chemistry and biology of macromolecular solutions. In spite of the fact, that this notation has not an explicit geometrical interpretation, it coincides unambiguously with the strictly defined extra void volume $V_B - V_B^{S,bulk}$, created in the boundary between solute and solvent [1,47]. Finally, it has to be stressed, that this extra void region, which determines the apparent volume is very short ranged, less than the extent of the first Delaunay shell.

The situation can be different for other solute molecules. In the analyzed simulations, the hIAPP molecule is in an "essentially random coil" state [56]. For larger, folded proteins a possible temperature-dependence of V_M has to be taken into account as well, because of internal extra voids. The different strengths of hydrophilicity or -phobicity of the solute molecule can also play a role.

To conclude, we hope that our results shine some light on the long-standing and often controversial debate surrounding the physical basis for understanding and decomposing the volumetric properties of biomolecular systems. Our results clearly support the notion that partial molar volumetric properties of peptides are strongly coupled to the volumetric properties (void volume) at the protein–solvent interface as well as to changes of the hydrational properties at the interface with respect to the bulk properties of the solvent. The conceptual basis for resolving volumetric properties into their various structural, interfacial and hydrational contributions using the approach presented might even enable us to unravel the various volumetric contributions of more complex systems and processes, such as natively folded proteins and protein–ligand interactions.

Acknowledgments

Financial support from Alexander von Humboldt foundation, grants from RFFI (No. 12-03-00654) and DFG (Cluster of Excellence RESOLV (EXC 1069)) are gratefully acknowledged. We thank Dr. M. Andrews for providing us with the trajectories of his hIAPP simulations.

References

[1] T.V. Chalikian, Volumetric properties of proteins, Annu. Rev. Biophys. Biomol. Struct. 32 (2003) 207–235.
[2] R. Winter, D. Lopes, S. Grudzielanek, K. Vogtt, Towards an understanding of the temperature/pressure configurational and free-energy landscape of biomolecules, J. Non-Equilib. Thermodyn. 32 (2007) 41–97.
[3] R. Mishra, R. Winter, Cold- and pressure-induced dissociation of protein aggregates and amyloid fibrils, Angew. Chem. Int. Ed. 47 (2008) 6518–6521.
[4] C. Royer, R. Winter, Protein hydration and volumetric properties, Curr. Opin. Colloid Interface Sci. 16 (2011) 568–571.
[5] D. Paschek, S. Nonn, A. Geiger, Low-temperature and high-pressure induced swelling of a hydrophobic polymer chain, in aqueous solution, Phys. Chem. Chem. Phys. 7 (2005) 2780–2786.
[6] W.F. van Gunsteren, D. Bakowies, R. Baron, I. Chandrasekhar, M. Christen, X. Daura, P. Gee, D.P. Geerke, A. Glättli, P.H. Hünenberger, C. Oostenbrink, M. Schenk, D. Trzesniak, N.F. van der Vegt, H.B. Yu, Biomolecular modeling: goals, problems, perspectives, Angew. Chem. Int. Ed. 45 (2006) 4064–4092.
[7] D. van der Spoel, E. Lindahl, B. Hess, G. Groenhof, A.E. Mark, H.J.C. Berendsen, GROMACS: fast, flexible, and free, J. Comput. Chem. 26 (2005) 1701–1718.
[8] N.N. Medvedev, Computational porosimetry, in: P. Engel, H. Syta (Eds.), Voronoi's Impact on Modern Science, Institute of Mathematics, National Acad. of Sciences of Ukraine, Kiev, 1998, pp. 165–175.
[9] S. Sastry, T.M. Truskett, P.G. Debenedetti, S. Torquato, F.H. Stillinger, Free volume in the hard-sphere liquid, Mol. Phys. 95 (1998) 289–297.
[10] G. Malavasi, M.C. Menziani, A. Pedone, U. Segre, Void size distribution in MD-modelled silica glass structures, J. Non-Cryst. Solids 352 (2006) 285–296.
[11] S. Rémond, J.L. Gallias, A. Mizrahi, Characterization of voids in spherical particle systems by Delaunay empty spheres, Granul. Matter 10 (2008) 329–334.
[12] M.D. Haw, Void structure and cage fluctuations in simulations of concentrated suspensions, Soft Matter 2 (2006) 950–956.
[13] B.J. Sung, A. Yethiraj, Structure of void space in polymer solutions, Phys. Rev. E. 81 (2010) 031801.
[14] M.G. Alinchenko, A.V. Anikeenko, N.N. Medvedev, V.P. Voloshin, M. Mezei, P. Jedlovszky, Morphology of voids in molecular systems. A Voronoi–Delaunay analysis of a simulated DMPC membrane, J. Phys. Chem. B 108 (2004) 19056–19067.
[15] H. Edelsbrunner, M. Facello, J. Liang, On the definition and construction of pockets in macromolecules, Discret. Appl. Math. 88 (1998) 83–102.
[16] J. Liang, H. Edelsbrunner, P. Fu, P. Sudhakar, S. Subramaniam, Analytical shape computation of macromolecules: II. Inaccessible cavities in proteins, Proteins Struct. Funct. Genet. 33 (1998) 18–29.
[17] D. Kim, C.-H. Cho, Y. Cho, J. Ryu, J. Bhak, D.-S. Kim, Pocket extraction on proteins via the Voronoi diagram of spheres, J. Mol. Graph. Model. 26 (2008) 1104–1112.
[18] T.M. Raschke, M. Levitt, Nonpolar solutes enhance water structure within hydration shells while reducing interactions between them, PNAS 102 (2005) 6777–6782.
[19] C. Schröder, T. Rudas, S. Boresch, O. Steinhauser, Simulation studies of the protein–water interface. I. Properties at the molecular resolution, J. Chem. Phys. 124 (2006) 234907.
[20] B. Bouvier, R. Grünberg, M. Nilges, F. Cazals, Shelling the Voronoi interface of protein–protein complexes predicts residue activity and conservation, Proteins Struct. Funct. Genet. 76 (2008) 677–692.
[21] G. Neumayr, T. Rudas, O. Steinhauser, Global and local Voronoi analysis of solvation shells of proteins, J. Chem. Phys. 133 (2010) 084108.
[22] A.V. Kim, V.P. Voloshin, N.N. Medvedev, A. Geiger, Decomposition of a protein solution into Voronoi shells and Delaunay layers: calculation of the volumetric properties, Trans. Comput. Sci. XX, Lect. Notes Comput. Sci 8110 (2013) 56–71.
[23] V.P. Voloshin, N.N. Medvedev, M.N. Andrews, R.R. Burri, R. Winter, A. Geiger, Volumetric properties of hydrated peptides: Voronoi–Delaunay analysis of molecular simulation runs, J. Phys. Chem. B 115 (2011) 14217–14228.
[24] A. Okabe, B. Boots, K. Sugihara, S. Chiu, Spatial tessellations—concepts and applications of Voronoi diagrams, John Wiley & Sons, New York, 2000.
[25] N.N. Medvedev, Voronoi–Delaunay Method for Non-crystalline Structures, Russian Academy of Science, Novosibirsk, 2000. (in Russian).
[26] F.M. Richards, The Interpretation of Protein Structures: Total Volume, Group Volume Distributions and Packing Density, J. Mol. Biol. 82 (1974) 1–14;
Calculation of Molecular Volumes and Areas for Structures of Known Geometry, Methods Enzymol. 115 (1985) 440–464.
[27] E.E. David, C.W. David, Voronoi polyhedra as a tool for studying solvation structures, J. Chem. Phys. 76 (1983) 4611–4614.
[28] B.J. Gellatly, J.L. Finney, Calculation of protein volumes: an alternative to the Voronoi procedure, J. Mol. Biol. 161 (1982) 305–322.
[29] P. Procacci, R. Scateni, A general algorithm for computing Voronoi volumes: application to the hydrated crystal of myoglobin, Int. J. Quantum Chem. 42 (1992) 1515–1528.
[30] M. Marchi, Compressibility of cavities and biological water from Voronoi volumes in hydrated proteins, J. Phys. Chem. B 107 (2003) 6598–6602.
[31] R.K. Singh, A. Tropsha, I.I. Vaisman, Delaunay tessellation of proteins: four body nearest neighbor propensities of amino acid residues, J. Comput. Biol. 3 (1996) 213–222.
[32] H. Edelsbrunner, E.P. Muecke, Three-dimensional alpha shape, ACM Trans. Graph. 13 (1994) 43–72.
[33] S.V. Anishchik, N.N. Medvedev, Three-dimensional Apollonian packing as a model for dense granular systems, Phys. Rev. Lett. 75 (1995) 4314–4317.
[34] N.N. Medvedev, V.P. Voloshin, V.A. Luchnikov, M.L. Gavrilova, An algorithm for three-dimensional Voronoi S-network, J. Comput. Chem. 27 (2006) 1676–1692.
[35] G.F. Voronoi, Deuxieme memoire: Recherches sur les paralleloedres primitifs, J. Reine Angew. Math. 136 (1909) 67–181.
[36] B.N. Delaunay, Sur la sphère vide. A la memoire de Georges Voronoi, Izv. Akad. Nauk SSSR, Otd. Mat. i Estestv. Nauk 7 (1934) 793–800.
[37] D.-S. Kim, Y. Cho, K. Sugihara, Quasi-worlds and quasi-operators on quasi-triangulations, Comput. Aided Des. 42 (2010) 874–888.

[38] F. Aurenhammer, Power diagrams: properties, algorithms and applications, SIAM J. Comput. 16 (1987) 78–96.
[39] V.P. Voloshin, N.N. Medvedev, A. Geiger, Fast calculation of the empty volume in molecular systems by the use of Voronoi–Delaunay sub simplexes, Trans. Comput. Sci., Lect. Notes Comput. Sci. 8360 (2014) 156–172.
[40] Computational Geometry Algorithms Library (CGAL,), http://www.cgal.org .
[41] T. Aste, K.Y. Szeto, W.Y. Tam, Statistical properties and shell analysis in random cellular structures, Phys. Rev. E 54 (1996) 5482–5492.
[42] M.N. Andrews, R. Winter, Comparing the structural properties of human and rat islet amyloid polypeptide by MD computer simulations, Biophys. Chem. 156 (2011) 43–50.
[43] C. Vega, J.L. Abascal, Relation between the melting temperature and the temperature of maximum density for the most common water models, J. Chem. Phys. 123 (2005) 144504.
[44] V.P. Voloshin, A.V. Anikeenko, N.N. Medvedev, A. Geiger, D. Stoyan, Hydration Shells in Voronoi Tessellations, Proc. 7-th Int. Symp. on Voronoi Diagrams in Science and Engineering, Quebec, Canada, June 2010, pp. 254–259.
[45] M.J. Blandemer, M.I. Davis, G. Douhéret, J.C.R. Reis, Apparent molar isentropic compressions and expansions of solutions, Chem. Soc. Rev. 30 (2001) 8–15.
[46] L. Mitra, N. Smolin, R. Ravindra, C. Royer, R. Winter, Pressure perturbation calorimetric study of the solvation properties and the thermal unfolding of proteins in solution—experiment and theoretical interpretation, Phys. Chem. Chem. Phys. 8 (2006) 1249–1265.
[47] T. Imai, Molecular theory of partial molar volume and its application to biomolecular systems, Condens. Matter Phys. 10 (3) (2007) 343–361.
[48] N.N. Medvedev, V.P. Voloshin, A.V. Kim, A.V. Anikeenko, A. Geiger, Calculation of the Partial Molar Volume and its Components on the Molecular Dynamics Models of Diluted Solutions, Zh. Strukt. Khim. 54 (2013) S90–S107 ((in Russian); English translation in J. Struct. Chem. 2014, in press).
[49] A.V. Kim, N.N. Medvedev, A. Geiger, Molecular dynamics study of the volumetric and hydrophobic properties of the amphiphilic molecule C8E6, J. Mol. Liq. 189 (2013) 74–80.
[50] R.A. Pierotti, Aqueous solutions of nonpolar gases, J. Phys. Chem. 69 (1965) 281–288.
[51] D.P. Kharakoz, Partial molar volumes of molecules of arbitrary shape and the effect of hydrogen bonding with water, J. Solut. Chem. 21 (1992) 569–595.
[52] N. Patel, D.N. Dubins, R. Pomès, T.V. Chalikian, Parsing partial molar volumes of small molecules: a molecular dynamics study, J. Phys. Chem. B 115 (2011) 4856–4862.
[53] M.J. Connolly, Analytical molecular surface calculation, J. Appl. Crystallogr. 16 (1983) 548–558.
[54] I. Brovchenko, M.N. Andrews, A. Oleinikova, Volumetric properties of human islet amyloid polypeptide in liquid water, Phys. Chem. Chem. Phys. 12 (2010) 4233–4238.
[55] A. Oleinikova, I. Brovchenko, R. Winter, Volumetric proprties of hydration water, J. Phys. Chem. C 113 (2009) 11110–11118.
[56] M.N. Andrews, R. Winter, Comparing the structural properties of human and rat islet amyloid polypeptide by MD computer simulations, Biophys. Chem. 156 (2011) 43–50.